3D mapping of lowland coastal peat domes in Indonesia

Earl C. Saxon[1,2], Sandra G. Neuzil[3], Dipo B.C. Biladi[4], Justin Kinser[5], Stuart M. Sheppard[2]

[1] Centre for Biodiversity and Conservation Science, University of Queensland, Saint Lucia QLD 4072, Australia
[2] Forest Inform Pty Ltd., 70 Drummond Street, Sinnamon Park QLD 4073, Australia
[3] US Geological Survey (Emerita), 12201 Sunrise Valley Drive, Reston VA 20192, USA
[4] PT EXSA Internasional, Jalan Tomang Raya No.74, Jakarta 11430, Indonesia
[5] Intermap Technologies, Inc., 8310 South Valley Highway # 400, Englewood CO 80112, USA

SUMMARY

Extent and thickness of peat deposits in Indonesia are poorly constrained although both are important factors in regulating peat use and in planning peat conservation. Innovations for mapping the extent and thickness of peat deposits were developed and tested on two highly disturbed peat domes on the islands of Sumatra and Kalimantan (Borneo), Indonesia. Peat dome surface topography was mapped by transforming radar Digital Surface Models (DSM) to Digital Terrain Models (DTM) using ortho-photogrammetric techniques and cadastral standard Ground Control Points (GCPs). Soil core samples were collected along gradient transects to determine the peat base topography. A digital peat base model (DPBM) was generated by fitting a surface to the peat base elevation points in soil cores. Combining the peat surface DTM with the peat base DPBM provides a three-dimensional model of peat extent and thickness. Maps derived from these models can inform a 'whole of dome' approach to resolving competing land use goals, reducing regional smoke hazard and mitigating greenhouse gas emissions. The DPBM makes a critical contribution to accurate peat dome mapping and successful peat management on Indonesia's coastal peatlands and in any other locations where peat has formed on an undulating irregular soil surface.

KEY WORDS: Digital Peat Base Model, gradient transect soil sampling, IFSAR DTM, peat thickness

INTRODUCTON

Indonesia's extensive peatlands store a substantial fraction of terrestrial carbon (Neuzil 1997, Page *et al.* 2011). Current uncertainties in the size of the Indonesian peat carbon pool are due to coarse estimations of both its extent - published areas range from 122,000 km^2 to 265,000 km^2 (Uda *et al.* 2017) - and its thickness (Wahyunto & Suryadiputra 2008, Page *et al.* 2011, Warren *et al.* 2017). The current extent and thickness of each peat dome reflects millennia of regional peat formation, decades of local land use change and years of site-specific burning.

As much as 80 % of western Indonesia's peat deposits, including both of the study sites discussed in this article, lie on coastal lowlands at elevations (altitudes) within a few metres of current mean sea level (Supardi *et al*. 1993, Dommain *et al.* 2014, Vernimmen *et al.* 2020). The topography of their bases undulate unpredictably, due to the interaction of climate and sea level fluctuations during the formation of those surfaces. For more than 100,000 years during the last glacial period, sea level was >120 m below current mean sea level. At that time the coastal lowlands of today were relatively elevated, inland and sub-aerially exposed. A combination of deposition, erosion and other soil forming processes shaped their surface soils (Supardi *et al.* 1993, Neuzil 1997, Dommain *et al.* 2014).

Between ~6,000 and ~4,000 years ago, post-glacial sea level rise peaked at ~5 m above current mean sea level, and this was accompanied by warmer and wetter weather in western Indonesia (Dommain *et al.* 2014). Today's coastal lowlands would have been almost entirely inundated, resulting in reworking and erosion of the previous soil surface. Sea level subsequently dropped and the local climate combined high annual rainfall (> 2.5 m yr^{-1}) with short dry seasons (< 3 months with rainfall ~100 mm month^{-1}) (Neuzil 1997, Dommain *et al.* 2014, Gaveau *et al.* 2014). These conditions supported peat deposition on coastal lowlands as falling sea levels exposed them (Supardi *et al.* 1993, Neuzil 1997, Dommain *et al.* 2014, Nasrul *et al.* 2020). Basal peat in coastal western Bengkalis Island has a radiocarbon date of 5860 cal BP (Dommain *et al*. 2011). Basal

peat deposition at Rasau Jaya, 30 km northwest of Kubu Raya, has five radiocarbon dates ranging from ~4500 cal BP to ~4300 cal BP (Ruwaimana *et al.* 2020).

Peatlands in Indonesia were largely undisturbed through the mid-1900s (Thorburn & Kull 2015), and Bengkalis Island was almost completely forested as recently as 1972 (Vernimmen *et al.* 2020). Following large scale land use change in the past four decades, these peatlands now support economic activities including industrial scale oil palm plantations, timber extraction and wood pulp production (Koh *et al.* 2011, Thorburn & Kull 2015, Miettinen *et al.* 2016, Uda *et al.* 2017), as well as smallholdings with coconuts, rubber and subsistence crops (Hergoualc'h & Verchot 2014, Thorburn & Kull 2015, Miettinen *et al.* 2016).

This has had collateral adverse effects (Thorburn & Kull 2015, Hergoualc'h *et al.* 2018). Natural undisturbed peat domes are waterlogged; the water table is near the surface of the peat and may fluctuate by a few tens of centimetres in response to the seasonal variations in rainfall (Dommain *et al.* 2010). Oil palm and acacia plantations thrive best when the water table is lowered to 50–75 cm below the peat surface throughout the year (Hooijer *et al.* 2015). This can be achieved only by artificial drainage, which rapidly deflates the peat and changes its surface topography (Hooijer *et al.* 2015, Evans *et al.* 2019, Tata 2019). Clearing peatland forests imperils wildlife (Posa *et al.* 2011, Husson *et al.* 2018). Draining and burning peatlands (Page *et al.* 2009, Miettinen *et al.* 2017) emit globally significant greenhouse gases (Gaveau *et al.* 2014, Hergoualc'h *et al.* 2018). Extensive peat fires produce stifling air pollution with airborne particulates that are a health hazard to humans and wildlife at a regional scale (Marlier *et al.* 2013, Crippa *et al.* 2016), and the dense lingering smoke has had substantial economic impacts over the entire region (Tacconi 2016, Lin *et al.* 2017).

The small area of remaining undisturbed peatland (Miettinen *et al.* 2016) plays a critical role in the conservation of peat swamp forest biodiversity (Posa *et al.* 2011, Husson *et al.* 2018).

Management of peatlands to achieve diverse goals - including economic development, regional air quality, community welfare, biodiversity conservation and mitigation of greenhouse gas emissions - requires detailed knowledge of the extent, shape, structure and condition of each peat dome. Government regulation of individual land holdings (Agus *et al.* 2012, Menteri Lingkungan Hidup dan Kehutanan 2017) on peatlands is especially difficult because each peat dome is a single, internally connected hydrological unit; actions that alter the water table in one part of the dome affect the whole dome (Jaenicke *et al.* 2010, Evans *et al.* 2019, Tata 2019) with severe long-term consequences (Hooijer *et al.* 2015, Wijedasa *et al.* 2017). Consequently, a 'whole of dome' approach (KFCP 2009, page 23) is needed to ensure that interventions which alter hydrology in one part of the dome do not have unintended adverse consequences elsewhere (Ichsan *et al.* 2013, Seymour & Samadhi 2018).

'Whole of dome' peatland management for multiple land uses requires detailed mapping of each peat dome's three-dimensional structure: its extent, thickness and stratification (Nasrul *et al.* 2020). The following five peat mapping methods - alone or in combination - are those most frequently implemented in Indonesia, with varying degrees of reliability:

- local schematic diagrams derived from soil profiles (Supardi *et al.* 1993, Agus *et al.* 2011);
- island-wide maps for Sumatra and Kalimantan, prepared from satellite imagery (Wahyunto & Suryadiputra 2008);
- topographic and land cover maps at scales of 1:50,000 and 1:250,000 prepared from air photographs (BIG 2018);
- regional maps prepared by combining surface topography from Light Detection and Ranging (LiDAR) strip sampling with soil core sample data to delineate the base topography comprising a lenticular rim and a flat centre (Hooijer & Vernimmen 2016, Siegert *et al.* 2018); and
- maps of individual peat domes derived from coarse digital elevation data and multi-temporal satellite imagery (Rudiyanto *et al.* 2018, Illés *et al.* 2019).

The conversion of peatlands from swamp forest to plantation cropping at the two study sites investigated here has altered the profile of each peat dome (Figure 1), creating challenges for mapping peat domes. Elevation data must be current, because peat dome topography changes rapidly in response to deforestation, peat surface levelling for plantations and deflation due to drainage and fires. Remote sensing data must be timely and processing techniques must be able to distinguish the peat soil surface from the clutter of vegetation, log piles, buildings, road embankments and drainage channels in order to determine the extant peat surface.

In this study, we developed a new method that creates detailed 3D maps of individual peat domes by combining radar remote sensing data, ground control points (GCPs) and strategic soil sampling along gradient transects. Interferometric Synthetic

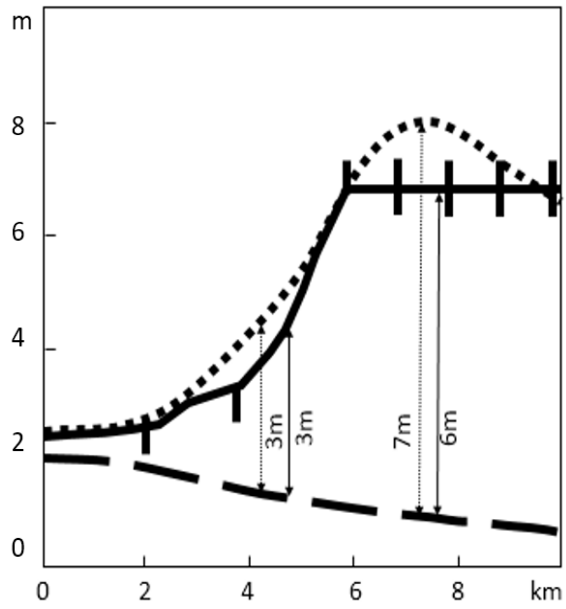

Figure 1. Schematic partial transect of a peat dome showing its original surface (dotted line), current surface (solid line) and peat base (long dashes). The location of isopachs (contours of equal peat thickness) are shown before (dotted line with arrows) and after (solid line with arrows) clearing, draining and crop planting. Deflation has increased the extent of peat < 3m deep - where regulations allow conversion of peatland. Roads and drains are indicated by vertical bars above and below the peat surface. Vertical exaggeration ×1000. Distances are measured from the edge of the peat dome (0.40 m isopach).

Aperture Radar (IFSAR) is a well-established remote sensing technology for obtaining high-resolution elevation data and corresponding ortho-rectified radar images of the earth's surface from airborne and space-borne platforms (Carswell 2013, Zakaria 2017). Unlike Landsat and LiDAR remote sensing systems operating at visible or near-infrared wavelengths, IFSAR systems use energy at microwave wavelengths to collect information about the terrain. This allows IFSAR to penetrate cloud cover, which is especially important in the tropics.

Our methodology was used to test assumptions underlying the five peat mapping methods currently in use. The 3D maps generated by this method can potentially be employed by the scientific community to reduce uncertainty in estimating the peat carbon pool, by government regulators to establish management boundaries based on peat thickness, and by planning officials to weigh options for mitigation of peatland fires, greenhouse gas emissions, peatland loss and flooding.

METHODS

Study sites

Two peat domes were mapped (Figure 2). The Bengkalis site occupies 55,800 ha in the eastern half of the Pulau Bengkalis *Kesatuan Hidrologis Gambut* (*KHG*) (= Peatland Hydrological Unit (PHU)) on Bengkalis Island, Riau Islands Province, adjacent to Sumatra. The Kubu Raya site comprises the entire Sungai Kapuas - Sungai Terentang *KHG* in Kabupaten Kubu Raya, West Kalimantan Province. It occupies a 23,400 ha island in the delta of the Kapuas River, Indonesia's longest river.

At both sites, the original forest cover has been lost due to logging, clearing and burning. Current land uses form a concentric pattern reflecting peat thickness. Small settlements and smallholder crop plots occupy the perimeter. Senescent coconut and rubber plantations occur on shallow peat. Industrial scale pulpwood and oil palm plantations extend across the deepest peat.

Digital terrain model (DTM) of the peat surface

At Bengkalis, Interferometric Synthetic Aperture Radar (IFSAR) data had been collected by Intermap Technologies, Inc. from an airborne platform in 2011, shortly after the natural tree cover was removed and uniform canopy plantations were established. These (X-band, 3 cm wavelength) data were suitable for post-processing into DTMs with a final pixel spacing of 5 m.

At Kubu Raya, Advanced Land Observing Satellite (ALOS) optical data were captured in 2014. These data have a 0.52 μm–0.77μm wavelength (Tadono *et al.* 2014) and the resulting elevation models have a pixel size of 30 m (Takaku *et al.* 2016). Intermap Technologies, Inc. utilised its Intelligent Resolution Improvement System (IRIS™) Digital Elevation Model (DEM) enhancement techniques (Mercer *et al.* 2018) to create a DSM elevation surface at a 5 m pixel spacing to emulate the resolution obtained from X-band IFSAR at Bengkalis.

IFSAR systems use two antennae separated by a fixed baseline to image the earth's surface by transmitting radar pulses toward the terrain. The reflected energy is recorded by both antennae simultaneously, providing the system with two Synthetic Aperture Radar (SAR) images (containing amplitude and phase data) of the same point on the ground, separated only by the phase difference created by the space between the two antennae. The phase difference between the antennae for each image point - along with range, baseline, GPS and navigation data - is used to infer the topographic height of the terrain being imaged. This enables the

creation of an interferogram (depicting the phase difference) from which the first-surface DSMs and Ortho-rectified Radar Images (ORIs) are derived (Richards 2007).

Unlike visible light, radar's microwave energy interacts with multiple layers in a vegetation canopy. Consequently, further processing is required to generate a bare soil DTM (Mercuri *et al.* 2006). Vegetation, buildings and other cultural features were digitally removed from the DSM to create the DTM in a semi-automated process using Intermap's proprietary 3D editing platform and software suite, leaving just the underlying terrain (Intermap Technologies, Inc. 2016, Rizaldy & Mayasari 2016). This method has been validated to have DTM accuracies of a similar order of magnitude to the DSMs, up to 1m RMSE in unobstructed areas with slopes < 10 degrees (Intermap Technologies, Inc. 2016).

Several features of deforested Indonesian peat domes lend themselves to such editing. The peat surface is virtually flat after draining and levelling for plantations, rectilinear plantations with irregular canopy heights have adjacent flat areas at regular intervals, narrow linear features such as drains and roads can be excluded from surface-fitting interpolation and artefacts such as log dumps and buildings are readily identifiable.

Trimble Global Navigation Satellite System stations with Trimble Zephyr Geodetic 2 antennas were deployed to establish new permanent geodetic survey stations within government precincts in the towns of Bengkalis (August 2016) and in Pontianak (August 2017), near the Bengkalis and Kubu Raya

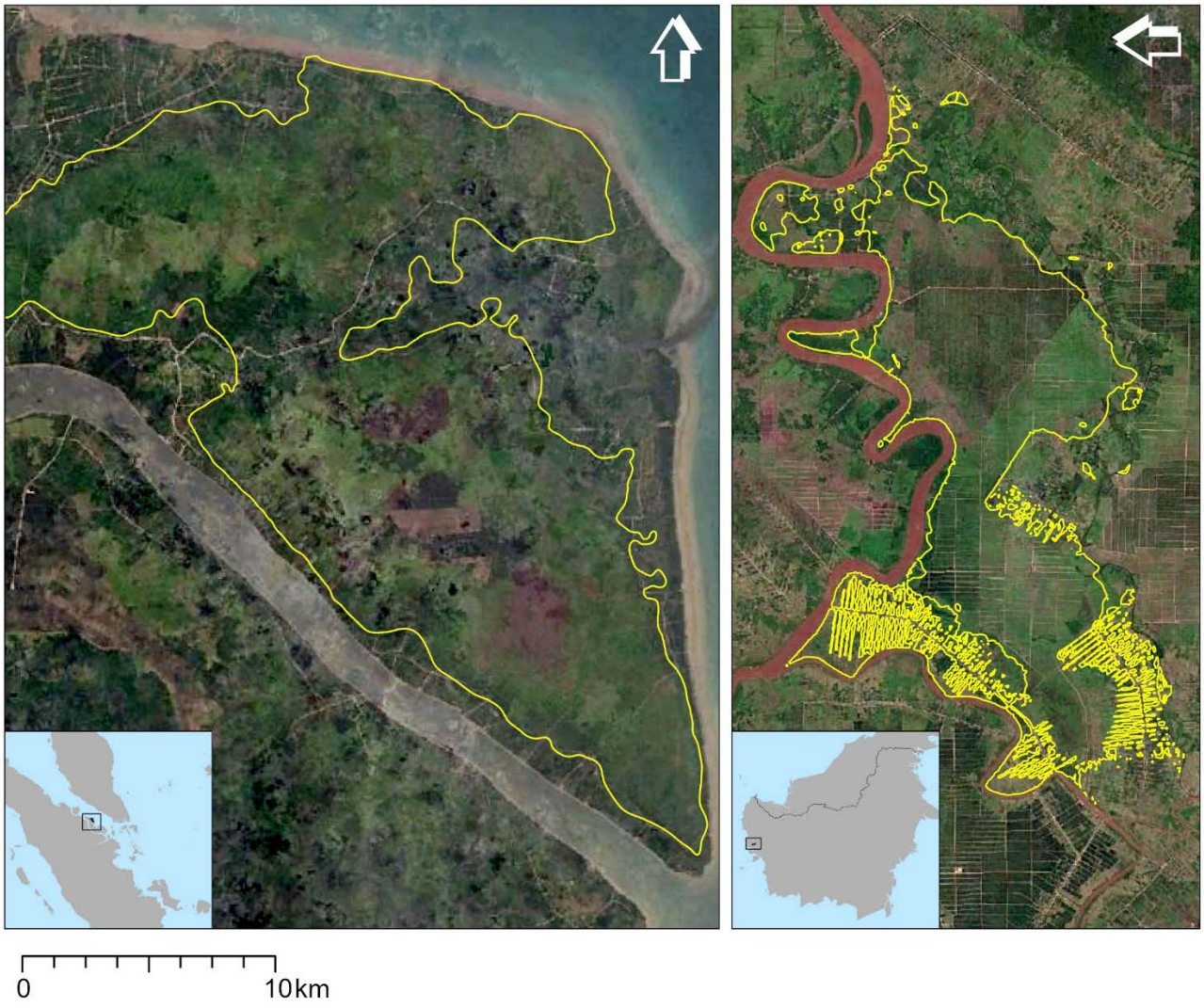

Figure 2. Extent of peat, bounded by the 0.40 m peat thickness isopach (yellow line), at the Bengkalis (left) and Kubu Raya (right) sites in Indonesia. At Kubu Raya, peat deflation following drainage and small cropping created a highly convoluted boundary. Elsewhere, the boundary is not aligned with any land use or land cover distinction visible in the satellite imagery.

study sites. Each station was referenced to Indonesia's national geodetic network with a horizontal accuracy of 0.01 m and vertical accuracy of 0.03 m. The same equipment was used to establish temporary GCPs in regularly spaced arrays across each site; 20 at Bengkalis and 26 at Kubu Raya (Figure 3). The location of each temporary GCP was determined by reference to geo-stationary satellites and to the new permanent geodetic survey station nearby. Wherever possible, a field GCP was established on an elevated bridge, culvert or building and offsets were measured to the adjacent peat surface. If no permanent landmark was available, the GCP was established on dry peat soil in a plantation

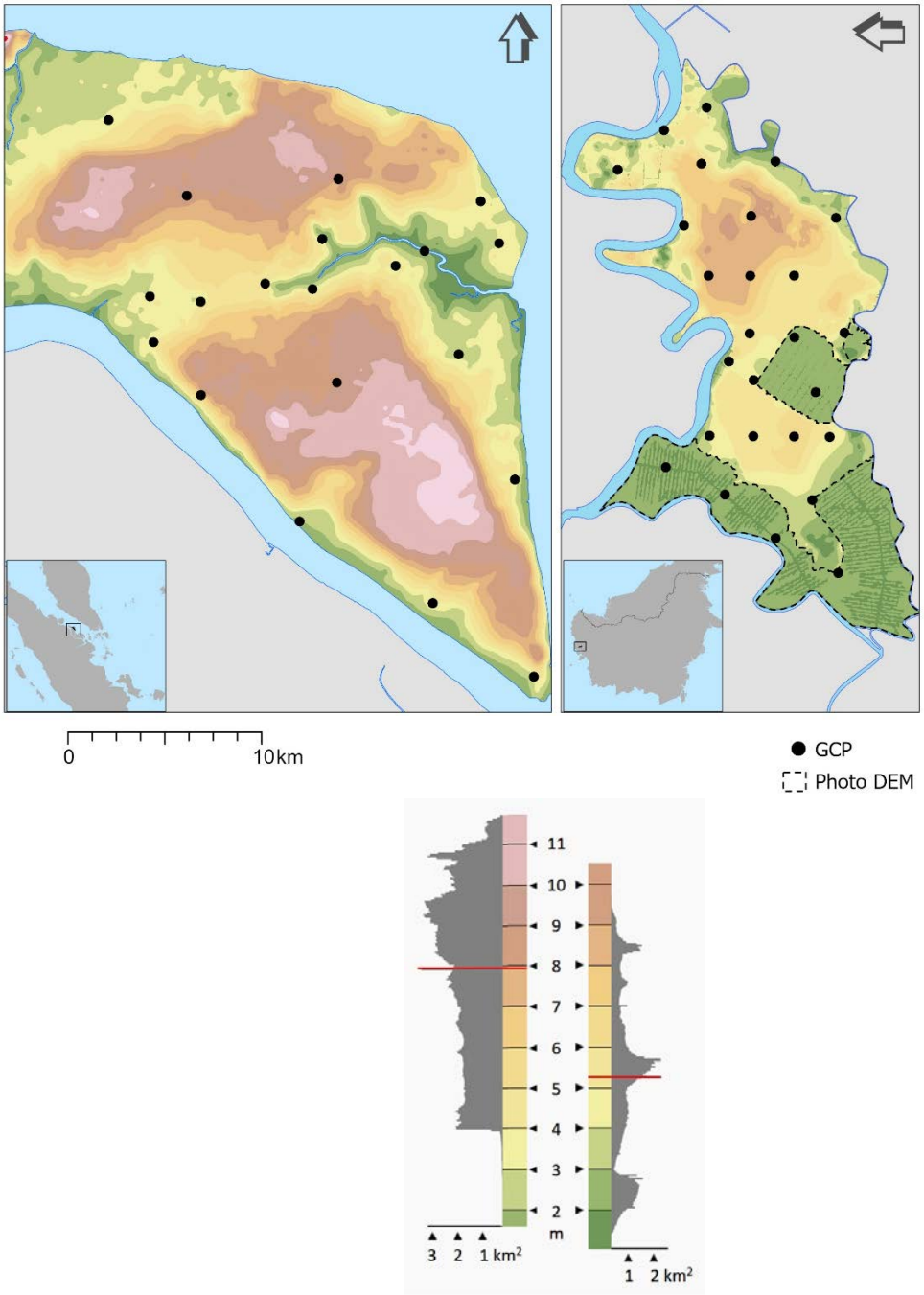

Figure 3. Ground Control Points (GCPs), peat surface elevation (m), peat extent at each surface elevation level (km^2) and mean surface elevation (red line) at Bengkalis (left) and Kubu Raya (right). At Bengkalis, coastal erosion has removed peat below 4 m. Bengkalis DTM is derived from airborne IFSAR. Kubu Raya DTM is derived from satellite SAR for higher elevations and from ortho-photogrammetric data at lower elevations (within dashed lines).

area, avoiding areas of obvious recent subsidence associated with drainage or fire.

The GCPs were used both to tie the draft DTM to national mapping standards and to update the provisional DTM, as follows:

- GCPs were used as reference points to assist in the removal of non-terrain surfaces such as stockpiled tree trunks, buildings and other cultural features observed in the radar data;

- GCPs in forested areas were referenced to assist in the estimation of local canopy height for the transformation from DSM to DTM; and

- GCPs in open areas were referenced to ensure the DTM was hydrologically sound for the peat surface DTM mapping.

Finally, during the re-edit of the DTM, any artefacts introduced during the automated DTM terrain-building process (e.g. swales beside drainage canals and abrupt break lines due to non-terrain surfaces) were removed. Statistics for the accuracy of the final DTM at each site are provided in Tables A1 and A2 in the Appendix.

Peat thickness in soil core samples

At Bengkalis, soil core samples were collected at 42 locations during two weeks in August–September 2016 and 52 locations during two weeks in April 2017. Additional data from 116 sites, sampled in 2014 for the Indonesian Department of Environment, were provided by the *Badan Informasi Geospasial* (*BIG*; Geospatial Information Agency). During two weeks in August 2017, soil core samples were collected at 152 locations at Kubu Raya (Figure 4).

In order to maximise information gained by each additional soil sample, soil core samples were obtained along multiple gradient transects running continuously from the deepest to the shallowest peat (Gillison & Brewer 1985). Each gradient transect followed the shortest feasible line, subject to the constraints of on-ground access and the interests of land owners and community members. Gradient transects were widely distributed across each site to capture variation in topography, edaphic factors and soil stratigraphy.

Soil core samples were obtained using stainless steel gouge augers (Eijkelkamp Soil & Water, Netherlands). On mineral soils adjacent to the peat domes, samples were obtained to a depth of 1.20 m to confirm that there was no shallow buried peat within sediments that may have encroached on the peat dome. On peat soil, sampling continued until mineral soil was encountered at the base of the peat. The thickest peat sampled was 10.40 m deep. Each peat layer in each soil core sample was characterised as saprist, hemist or fibrist according to the degree of decomposition of its organic matter content (FAO 2018). Representative soil samples were archived.

Digital peat base model (DPBM)

The elevation of the base of the peat at each soil core sample was determined by subtracting peat thickness from elevation of the peat surface in the DTM. ArcGIS Topo Point to Raster tool (ESRI, Redlands CA, USA) was used to interpolate a continuous, hydrologically sound raster grid from the peat base elevation point data (Figure 4). While both the peat surface DTM and the soil samples were time-consuming and expensive to obtain, digital processing of these data to create a peat base DPBM required neither significant preparation time nor cost.

3D model

Peat thickness was modelled as the difference between the continuous surface DTM and the continuous base DPBM. The extent of the peat dome was truncated where the difference between the upper and lower modelled surfaces was 0.4 m, following the standard soil classification protocol (FAO 2018).

Two error terms were calculated for the model: surface fitting error and sampling error. Surface fitting error is the discrepancy between peat thickness measured at the soil sampling points and peat thickness calculated in the model at the same points. Sampling error is the difference between average peat thickness at soil sampling points in the model and average peat thickness across the entire surface interpolated from those points.

RESULTS

Peat thickness in soil core samples

Peat thickness in the soil core samples links the peat surface DTM with the peat base DPBM. The thickness, surface elevation, base elevation and internal stratification of the soil samples can be visualised simultaneously as a 3D model, viewable from any angle (Figure 5). The core samples confirm that peat thickness varies unpredictably and does not necessarily conform to the conventional lenticular model. For example, peat is very deep at the southwest edge of the Bengkalis peat dome. In narrow sections linking sub-domes, it can be either deep (e.g. Bengkalis) or shallow (e.g. Kubu Raya). Consequently, simple peat models that extrapolate peat thickness from distance to the edge of the peat dome would be invalid at these sites.

Digital terrain model (DTM) of the peat surface

Sub-metre elevation accuracy of the IFSAR peat surface DTM after adjustment to the GCPs was achieved at both Bengkalis (RMSE = 0.229 m) (Table A1) and Kubu Raya (RMSE = 0.074 m) (Table A2). Reliance on existing IFSAR, ALOS and ortho-photogrammetric data allowed this study to compile peat surface DTMs rapidly at low cost.

Digital peat base model (DPBM)

Sub-metre elevation accuracy of the peat base DPBM was achieved at both Bengkalis (RMSE = 0.129 m among 121 core samples with peat) and Kubu Raya (RMSE = 0.024 m among 109 core samples with peat). At both sites, the average elevation of the base in deep peat (peat > 3.0 m thick) was found to be lower than in shallow peat (peat 0.40–3.0 m thick)

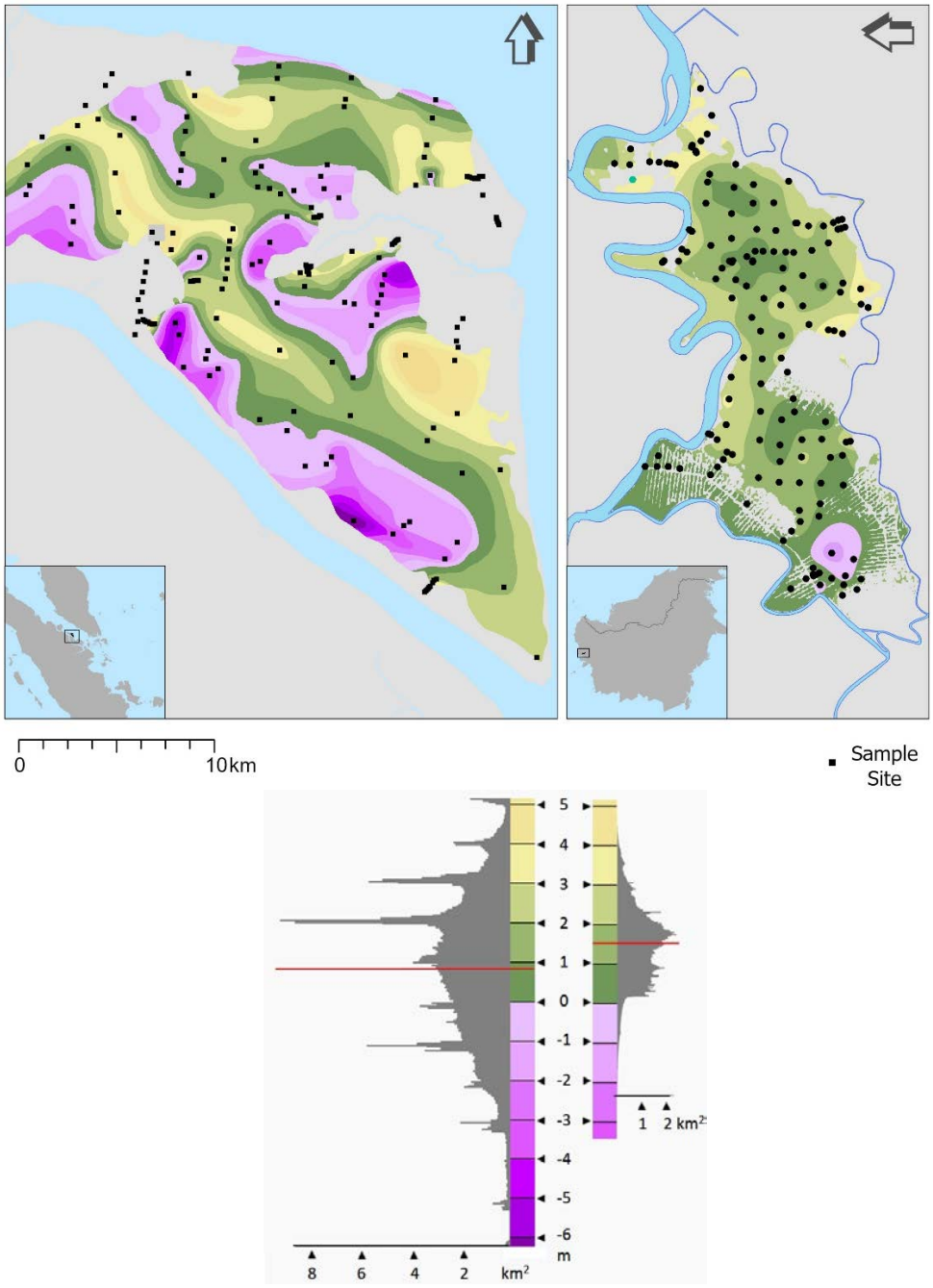

Figure 4. Soil sample points, peat base elevation (m), peat extent at each base elevation level (km^2) and mean peat base elevation (red line) at Bengkalis (left) and Kubu Raya (right). At Bengkalis, peaks in the frequency of peat base area at distinct intervals may indicate extensive mud flats on the pre-deposition surface due to coastal erosion and sea level fluctuations.

(Table 1), consistent with the conventional lenticular model of a peat dome. However, elevation of the peat base is highly variable, reflecting the relict topography before peat was deposited (Nasrul *et al.* 2020). Mapping the extent of the peat base that is currently below or slightly above mean sea level provides a basis for estimating risk of anaerobic peat deflation compared to fire and aerobic peat deflation in areas significantly above mean sea level.

3D model

Subtracting the peat base DPBM from the peat surface DTM allows peat area and volume to be calculated (Table 2) and mapped (Figure 6). Sub-metre RMSE was obtained for surface fitting error (Table A3). Sub-metre RMSE and low z-scores were obtained for sampling error (Table A4).

Variations in base topography (Figure 4), due to the combination of sub-aerial formation and marine

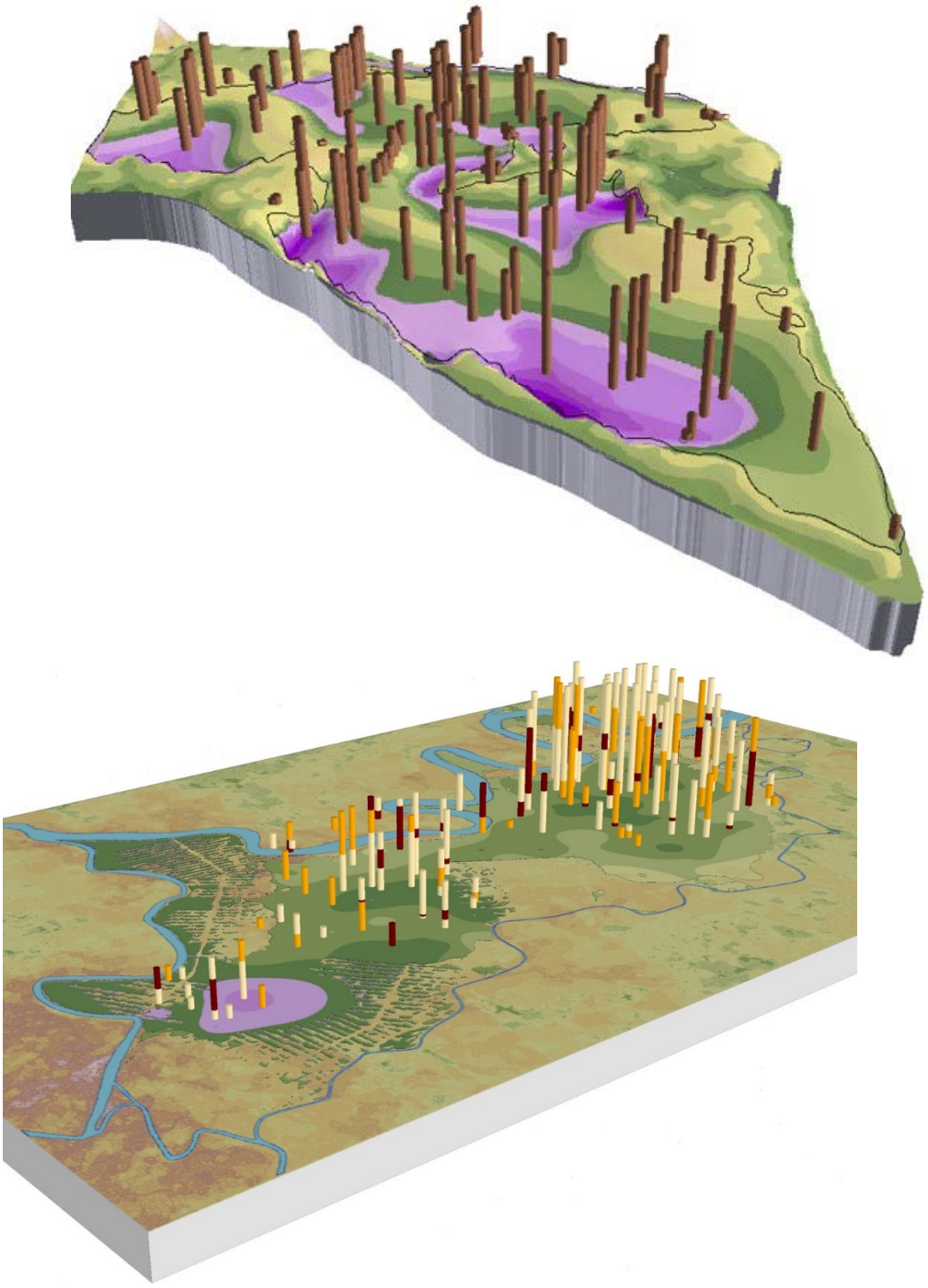

Figure 5. 3D Visualisations of peat base elevation (see Figure 4 for legend) at Bengkalis (above), with measured peat thickness in soil cores and at Kubu Raya (below), with measured thickness of individual saprist, hemist or fibrist peat soil strata observed in core samples).

Table 1. Average elevation (m above MSL) of the peat base with shallow peat (0.4–3.0 m thick) and deep peat (> 3.0 m thick) in soil cores.

Location	Peat thickness	No. of cores	Average elevation
Bengkalis	shallow	34	3.02 ± 0.76
	deep	88	-0.24 ± 2.26
Kubu Raya	shallow	60	2.01 ± 1.45
	deep	49	1.21 ± 0.76

Table 2. Peat extent and volume for shallow peat (0.4–3.0 m thick) and deep peat (> 3.0 m thick) based on the 3D Model.

Location	Peat thickness	Peat area (ha)	Peat volume (1,000,000 m^3)
Bengkalis	shallow	3,783	69
	deep	34,763	2,657
Kubu Raya	shallow	9,672	143
	deep	5,690	276

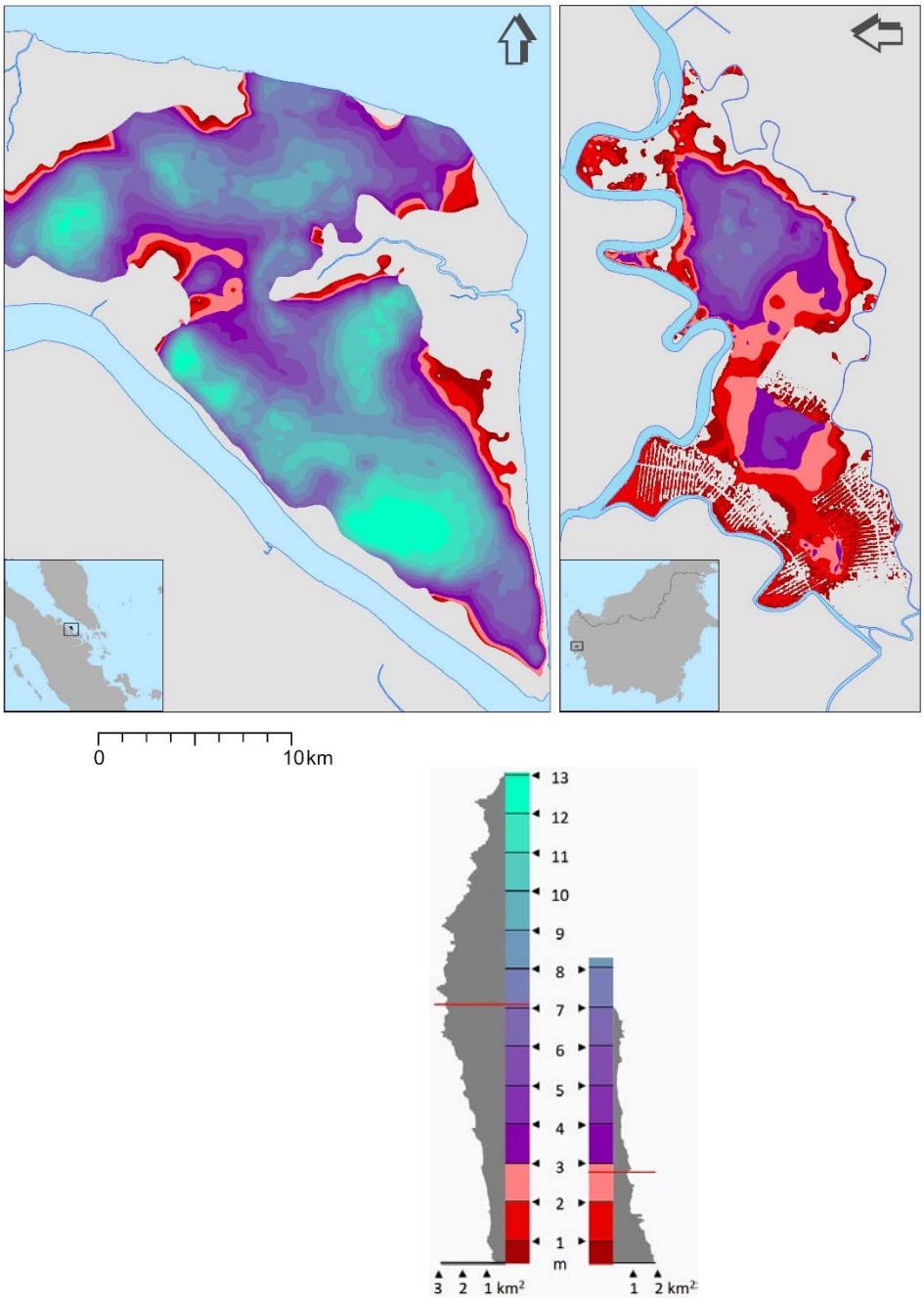

Figure 6. Peat thickness (m), peat extent at each thickness level (km^2) and mean thickness (red line) at Bengkalis (left) and Kubu Raya (right). At Kubu Raya, drainage, levelling and deflation have created a higher ratio of shallow peat to deep peat compared with Bengkalis.

transgressions, reflect drainage patterns established before peat formation. Variations in surface topography (Figure 5), are due to a combination of levelling, draining, planting, deflation and burning, reflecting highly localised patterns of recent land use and land use change. Given their different formation periods and formative processes, there is no correlation between the elevations of the two surfaces (Bengkalis R^2 = 0.000 in 111 cores, Kubu Raya R^2 = 0.011 in 109 cores). In combination, the uncorrelated base relief and surface relief create noisy frequency patterns in the distribution of peat thickness within sites and distinctive differences between them (Figure 6).

DISCUSSION

The detailed measurements at Bengkalis and Kubu Raya demonstrate inconsistencies with several of the assumptions currently used to simplify the tasks of mapping peat extent and thickness, estimating carbon content of peatlands and prioritising sites for protection and restoration of peat swamp forests.

Peat maps based on distance from the nearest water body (Giesen *et al*. 2013) or based on soil transects (Agus *et al.* 2011) allocate half the observed peat thickness to above the elevation of the surrounding mineral soil and half to below-ground. Our 3D maps at Bengkalis and Kubu Raya show that the surface DTM and the peat base DPBM are not symmetrical (Figure 3, Figure 4).

Peat maps based on satellite or air photographic observation of land cover assume that boundaries between land cover types are associated with the boundary between mineral and peat soils and the boundary between shallow and deep peat, respectively the 0.4 m and 3.0 m isopachs (Wahyunto & Suryadiputra 2008). Our methodology, confirmed by on-ground observations, demonstrates that boundaries between natural land cover and areas with commercial plantations or small-scale crops are not aligned with peat thickness isopachs at Bengkalis (Figure 7).

Peat maps based on detailed surface elevation data, combined with a limited set of soil thickness measurements, rely on the simplifying assumptions that the peat surface is lenticular and that the peat base is lenticular at its margin, but otherwise flat and at a consistent average elevation in relation to sea level (Hooijer & Vernimmen 2016, Siegert *et al.* 2018, Vernimmen *et al.* 2020). At Bengkalis and Kubu Raya, neither of these assumptions is valid.

Given our findings that the average elevation of the peat base in deep peat (> 3.0 m thick) was lower than in shallow peat (0.4–3.0 m thick), any maps based on the average peat base elevation of the entire dome would under-estimate the thickness and volume of deep peat and over-estimate the thickness and volume of shallow peat. Under-estimation of the thickness of deep peat creates erroneous mapping extensions of shallow peat on which government regulations allow conversion of peat swamp forest to plantations.

Accurate mapping of the peat surface is critical for managing and monitoring peat deflation. When natural peat swamp forest is disturbed drastically by logging, drainage and plantations, there will be an ongoing net loss of peat, even under best management practices (Wijedasa *et al.* 2017). Peat collapse, compaction, decomposition and fire lower peat surface elevation, eventually reaching a slope gradient < 0.2 m km^{-1}. At that point, peat no longer drains; it becomes permanently inundated (Hooijer *et al.* 2015) and unsuitable for plantation crops. Some smallholding crops, for example sago, may be viable in these conditions (Thorburn & Kull 2015, Tata 2019). 3D mapping detected extensive areas of surface deflation at both sites, where drained plantations had been burned and abandoned. Such occurrences near sea level on the coast are subject to tidal flooding, salt water intrusion (Hooijer *et al.* 2015, Thorburn & Kull 2015) or rapid erosion of the remaining peat layer (Sutikno *et al.* 2017).

Detailed topographic maps of the peat base reveal the geomorphology of a fossil land surface from the time when peat formation halted any erosion, deposition and other soil forming processes that previously shaped it (Supardi *et al.* 1993, Nasrul *et al*. 2020). 3D topographic mapping of this buried pre-peatland surface (Figure 4) revealed relict formations created by interactions among sub-aerial processes, drainage, tidal forces and marine transgressions.

Where a combination of disturbances lowers the peat surface below high tide levels and the peat base is below current mean sea level, the depressions formed are especially susceptible to salt water intrusion, elevating the concentrations of dissolved salts and sulfates in the peat. Such a change in chemical conditions damages crops and may enhance methane emissions through anaerobic peat decay (Inubushi *et al.* 2003) or ultimately create acid sulfate soils unsuitable for agriculture (Andriesse & Van Mensvoort 2006). Furthermore, even slightly lowered topographic depressions and drainage pathways on the peat surface can become permanent shallow open water areas in the near term, through a combination of sea level rise, tidal-driven coastal erosion and deflation of the peat surface (Hooijer *et al.* 2015).

Plantations and drainage canals increase peat degradation at the peat surface and near canals (Nasrul *et al.* 2020), and thus lower the hydraulic conductivity. In combination, they can reduce the rate of rainfall infiltration into peat. Since water flow in peat domes is gravity driven (Dommain *et al.* 2010), knowledge of the elevation of the peat surface and of the individual layers within the peat are critical for predicting water flow paths and drainage rates through and out of a peat dome. Hydraulic conductivity of tropical peat may range from > 400 m d^{-1} in fibrous peat to as low as < 0.5 m d^{-1} in sapric peat (Dommain *et al.* 2010, Hooijer *et al.* 2015). Within the peat domes at Bengkalis and Kubu Raya, layers with different degradation vary in both thickness and elevation. Mapping this internal structure provides critical information for management practices needed to maintain a minimum depth to the water table in order to break the feedback processes that accelerate loss of carbon stocks (Wijedasa *et al.* 2017, Hergoualc'h *et al.* 2018) through peat deflation, fire, coastal erosion and enhanced anaerobic loss due to salt water intrusion.

It is likely that the enhanced DTM editing techniques, specifically relevant to peatland mapping, that were developed during this study can be applied to other remotely sensed data. Radar remote sensing data are becoming more widely available with satellites such as Sentinel-1 C-band and the Radarsat Constellation Mission (Zan & Guarnieri 2006, Dabboor *et al.* 2018). Wherever interferometric pairs of radar satellite images are available, DSMs can be generated and the DTM generation techniques employed here for peatland mapping can be utilised.

The combination of a detailed peat surface DTM with a detailed peat base DPBM provides maps of the peat dome's 0.4 m and 3.0 m isopachs (contours of

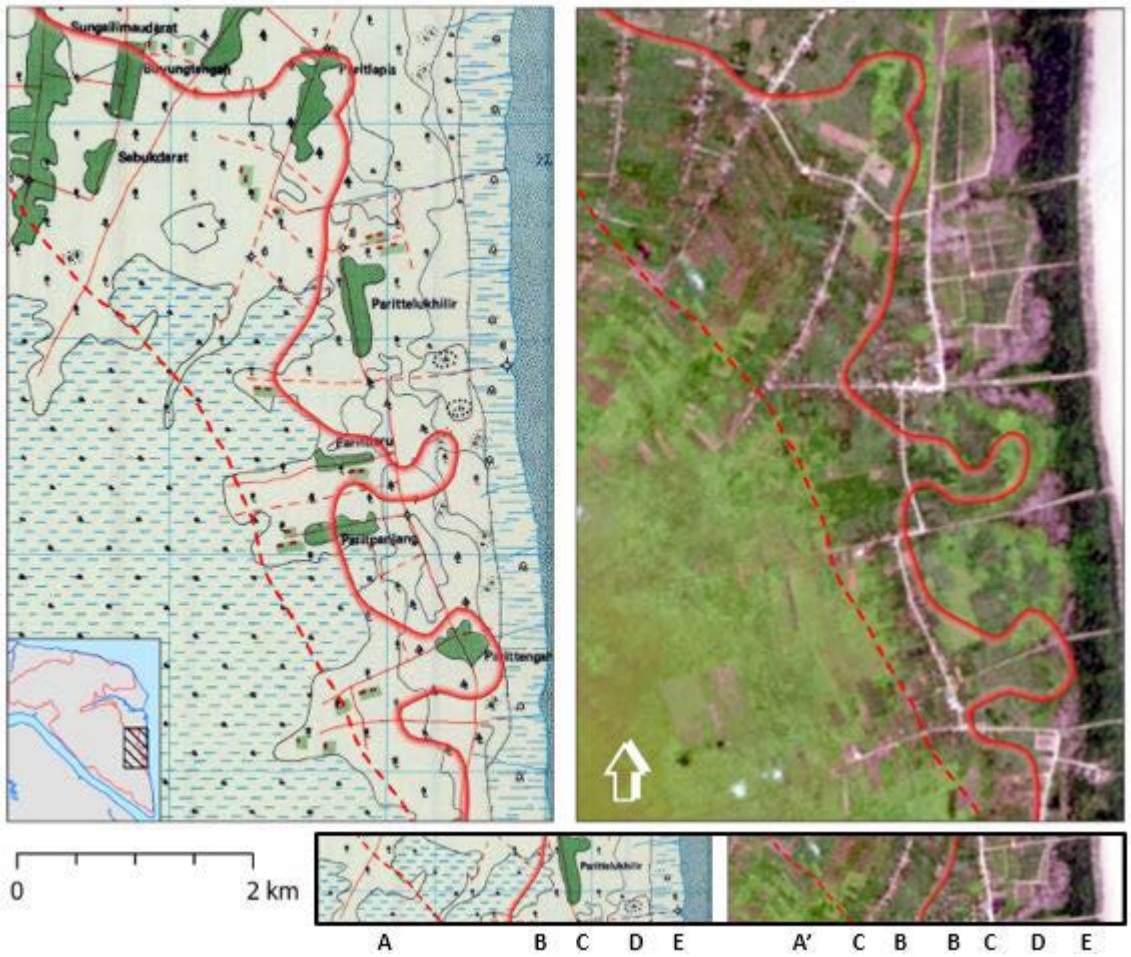

Figure 7. Comparison of the 0.40 m isopach (solid red line, perimeter of shallow peat) and the 3.0 m isopach (dashed red line, perimeter of deep peat) from this study with peat swamp (A), oil palm plantation (A'), mixed crops (B), settlements and roads (C), bare land (D) and mangroves (E) from the 1:50,000 scale topographic map (BIG 2018) (left) and Landsat 8 OLI 15 m multi-temporal Pansharpened Natural Color image (ESRI 2019) (right).

equal peat thickness), respectively the shallow peat boundary and the deep peat boundary under Indonesian peatland regulations.

Our methodology captures within-dome variation in elevation and peat thickness at a greater level of detail than conventional maps extrapolated from surface topography and limited soil sampling, particularly on coastal peat domes. These are less amenable to generalised modelling, given their combination of an irregular peat soil base (formed by post-glacial marine transgressions) with an irregular peat soil surface (formed by multiple, recent, drivers of peat loss). Integrating data from multiple sources (remote sensing of topography, geodetic surveys and gradient transect soil samples) delivers 3D mapping with sub-metre accuracy and quantified error terms. Since all parts of a peat dome are hydrologically connected, this level of detail is needed for effective management of the diverse processes that drive degradation, fires and greenhouse gas emissions from different parts of each peat dome. Without this level of detailed peat dome mapping, interventions and regulations may fail to deliver their intended outcomes and may also create unintended and irreversible collateral damage.

ACKNOWLEDGEMENTS

Access to field sites was authorised by national and provincial authorities and local land holders under the auspices of the Indonesian Peat Prize. The research project was managed by Titik Buryani and Ariffin Tjekiagus (PT EXSA Internasional), Justin Kinser (Intermap Technologies, Inc.) and Ester Saxon (Forest Inform Pty. Ltd). Darminto led the field and technical teams including Fitra Fitrotulhaq, Abdul Hasyim, Mulyadi, Syamsu Rizal, Davit Rudiasnyah and Achmad Tohari. Ernie DeCol led the data acquisition, processing and reporting team at Intermap Technology, Inc. The authors thank Ralph Dubayah, Beth Middleton, Daniel Murdiyarso, Sassan Saatchi, Lisamarie Windham-Myers and two anonymous reviewers for their constructive comments on manuscript drafts.

AUTHOR CONTRIBUTIONS

ECS integrated the field, remote sensing and GIS methods. SGN analysed the peat formation processes. DBCB led the soil surveys. JK coordinated the remote sensing and topographic mapping. SMS conducted the GIS analyses and produced the maps and Figures. All authors contributed to the final version of the article.

REFERENCES

Agus, F., Hairiah, K., Mulyani, A. (2011) *Measuring Carbon Stock in Peat Soils: Practical Guidelines*. World Agroforestry Centre (ICRAF) Southeast Asia Regional Program, Indonesian Centre for Agricultural Land Resources Research and Development, Bogor, Indonesia, 60 pp. Online at: http://www.worldagroforestry.org/downloads/Publications/PDFS/MN17335.PDF, accessed 30 Dec 2020.

Agus, F., Wahyunto, Dariah, A., Runtunuwu, E., Susanti, E., Supriatna, W. (2012) Emission reduction options for peatlands in the Kubu Raya and Pontianak Districts, West Kalimantan, Indonesia. *Journal of Oil Palm Research*, 24, 1378–1387.

Andriesse, W., Van Mensvoort, M.E.F. (2006) Acid sulfate soils: distribution and extent. In Lai, R. (ed.) *Encyclopedia of Soil Science*, 2nd edition, CRC Press, Boca Raton FL, 14–19.

BIG (2018) *Topographic Map*. Badan Informasi Geospasial (BIG) (Geospatial Information Agency). Online at: https://tanahair.indonesia.go.id/portal-web/downloadpetacetak?skala=50K, accessed 30 Dec 2020.

Carswell, W.J.Jr. (2013) *The 3D Elevation Program - Summary for Alaska*. USGS Fact Sheet 2013-3083, United States Geological Survey (USGS), 2 pp. Online at: https://pubs.usgs.gov/fs/2013/3083/pdf/fs2013-3083.pdf, accessed 29 Dec 2020.

Crippa, P., Castruccio, S., Archer-Nicholls, S., Lebron, G.B., Kuwata, M., Thota, A., Sumin, S., Butt, E., Wiedinmyer, C., Spracklen, D.V. (2016) Population exposure to hazardous air quality due to the 2015 fires in Equatorial Asia. *Scientific Reports*, 6, 37074, 9 pp.

Dabboor, M., Iris, S., Singhroy, V. (2018) The RADARSAT Constellation Mission in support of environmental applications. *Proceedings of the 2nd International Electronic Conference on Remote Sensing*, 2, 323, 5 pp.

Dommain, R., Couwenberg, J., Joosten, H. (2010) Hydrological self-regulation of domed peatlands in south-east Asia and consequences for conservation and restoration. Mires and Peat, 6, 05, 17 pp.

Dommain, R., Couwenberg, J., Joosten, H. (2011) Development and carbon sequestration of tropical peat domes in south-east Asia: links to post-glacial sea-level changes and Holocene climate variability. *Quaternary Science Reviews*, 30(7–8), 999–1010.

Dommain, R., Couwenberg, J., Glaser, P.H., Joosten, H., Suryadiputra, I.N.N. (2014) Carbon storage

and release in Indonesian peatlands since the last deglaciation. *Quaternary Science Reviews*, 97, 1–32.

ESRI (2019) Landsat 8 OLI 15 m Multi-temporal Pansharpened Natural Color images. Environmental Systems Research Institute (ESRI), Redlands, CA. (Online at: https://www.arcgis.com/home/item.html?id=c34fd380d16f40a7bb7995ac4d7ab8de

Evans, C.D., Williamson, J.M., Kacaribu, F., Irawan, D., Suardiwerianto, Y., Hidayat, M.F., Laurén, A., Page, S.E. (2019) Rates and spatial variability of peat subsidence in *Acacia* plantation and forest landscapes in Sumatra, Indonesia. *Geoderma*, 338, 410–421.

FAO (2018) *Key to the FAO Soil Units (1974): Histosols*. Soils Portal, Food and Agriculture Organization of the United Nations (FAO). Online at: http://www. fao.org/soils-portal/soil-survey/soil-classification/fao-legend/key-to-the-fao-soil-units/en/, accessed 29 Dec 2020.

Gaveau, D.L., Salim, M.A., Hergoualc'h, K., Locatelli, B., Sloan, S., Wooster, M., Marlier, M.E., Molidena, E., Yaen, H., DeFries, R., Verchot, L., Murdiyarso, D., Nasi, R., Holmgren, P., Sheil, D. (2014) Major atmospheric emissions from peat fires in Southeast Asia during non-drought years: evidence from the 2013 Sumatran fires. *Scientific Reports*, 4, 6112, 7 pp.

Giesen, W., Gevers, G.J.M., Ilman, M. (2013) *Policy Note on Mangroves & Tambak Development in Indonesia: Quick Assessment and Nationwide Screening (QANS) of Peat and Lowland Resources and Action Planning for the Implementation of a National Lowland Strategy*. Report PVW3A10002, Agentschap NL 6201068 QANS Lowland Development, Euroconsult Mott MacDonald, Deltares, Wageningen UR and partners, for Ministry of Public Works and BAPPENAS, Government of Indonesia and Partners for Water (Netherlands), 7 pp. Online at: https://edepot.wur.nl/251354, accessed 29 Dec 2020.

Gillison, A.N., Brewer, K.R.W. (1985) The use of gradient directed transects or gradsects in natural resource surveys. *Journal of Environmental Management*, 20, 103–127.

Hergoualc'h, K., Verchot, L.V. (2014) Greenhouse gas emission factors for land-use and land-use change in Southeast Asian peatlands. *Mitigation and Adaptation Strategies for Global Change*, 19(6), 789–807.

Hergoualc'h, K., Carmenta, R., Atmadja, S., Martius, C., Murdiyarso, D., Purnomo, H. (2018) *Managing Peatlands in Indonesia: Challenges and Opportunities for Local and Global Communities*. CIFOR Infobrief 205, 8 pp. Online at: https:// www.cifor.org/library/6449/, accessed 29 Dec 2020.

Hooijer, A., Vernimmen, R. (2016) Exploration of efficient and cost-effective use of LiDAR data in lowland/peatland landscape mapping and management in Indonesia. Deltares, Jakarta. (Online at: https://www.deltares.nl/en/projects/lidar-data-large-scale-peatland-management-flood-risk-assessment/, accessed 29 Dec 2020.

Hooijer, A., Vernimmen, R, Mawdsley, N., Page, S., Mulyadi, D., Visser, M. (2015) *Assessment of Impacts of Plantation Drainage on the Kampar Peninsula Peatland, Riau*. *Deltares Report* 1207384 to Wetlands International, CLUA and Norad, 80 pp. (Online at: https://www.yumpu.com/en/document/read/55429531/plantation-impacts-kampar-peatland-deltares-2015, accessed 29 Dec 2020.

Husson, S.J., Limin, S.H., Adul, Boyd, N.S. and 27 others (2018) Biodiversity of the Sebangau tropical peat swamp forest, Indonesian Borneo. *Mires and Peat*, 22, 05, 50 pp.

Ichsan, N., Vernimmen, R., Hooijer, A., Applegate, G. (2013) *KFCP Hydrology and Peat Monitoring Methodology*. Technical Paper, Kalimantan Forests and Climate Partnership, Indonesia-Australia Forest Carbon Partnership, Jakarta, 37 pp. Online at: https://www.forda-mof.org/files/6._KFCP_Hydrology_and_Peat_Monitoring_Methodology.pdf, accessed 29 Dec 2020.

Illés, G., Sutikno, G., Szatmári, G., Sandhyavitri, A., Pásztor, L., Kristijono, A., Molnár, G., Yusa, M., Székely, B. (2019) Facing the peat CO_2 threat: digital mapping of Indonesian peatlands - a proposed methodology and its application. *Journal of Soils and Sediments*, 19, 3663–3678.

Intermap Technologies, Inc. (2016) *Product Handbook & Quick Start Guide: Edit Rules Edition, v4.5*. Intermap Technologies, Inc., Denver, 152 pp. Online at: https://www.intermap.com/hubfs/pdf/brochures/INTERMAP%20-%20Product%20Handbook.pdf, accessed 29 Dec 2020.

Inubushi, K., Furukawa, Y., Hadi, A., Purnomo, E., Tsuruta, H. (2003) Seasonal changes of CO_2, CH_4 and N_2O fluxes in relation to land-use change in tropical peatlands located in coastal area of South Kalimantan. *Chemosphere*, 52(3), 603–608.

Jaenicke, J., Wosten, H., Budiman, A., Siegert, F. (2010) Planning hydrological restoration of peatlands in Indonesia to mitigate carbon dioxide emissions. *Mitigation and Adaptation Strategies for Global Change*, 3, 223–239.

KFCP (2009) *Kalimantan Forests and Climate Partnership (KFCP) Design Document*. Australia Indonesia Partnership, 133 pp. Online at: https://www.yumpu.com/en/document/read/31344274/kalimantan-forests-and-climate-partnership-kfcp-design-, accessed 29 Dec 2020.

Koh, L.P., Miettine, J., Liew, S.C., Ghazoula, J. (2011) Remotely sensed evidence of tropical peatland conversion to oil palm. *Proceedings of the National Academy of Sciences of the United States of America (PNAS)*, 108(12), 5127–5132.

Lin, Y., Wijedasa, L.S., Chisholm, R.A. (2017) Singapore's willingness to pay for mitigation of transboundary forest-fire haze from Indonesia. *Environmental Research Letters*, 12(2), 024017, 8 pp.

Marlier, M.E., DeFries, R.S., Voulgarakis, A., Kinney, P.L., Randerson, J.T., Shindell, D.T., Chen, Y., Faluvegi, G. (2013) El Niño and health risks from landscape fire emissions in southeast Asia. *Nature Climate Change*, 3(2), 131–136.

Menteri Lingkungan Hidup dan Kehutanan Republic Indonesia (Minister of Environment and Forestry of Republic Indonesia) (2017) Tentang peta indikatif arahan pemanfaatan hutan produksi yang tidak dibebani izin untuk usaha permanfaatan hutan (Decision on the indicative map of the use of production forest utilisation which is not burdened with permits for forest utilisation). Nomor: SK. 4732 / MenLHK-PHPL/ KPHP / HPL. 0/9/2017, 2017 (in Indonesian). Online at: https://drive.google.com/file/d/0B0WeKk7HPvj7V0QwTEhUeFhVc2M/view, accessed 29 Dec 2020.

Mercer, N.Z., Griffiths, S.C., Wollersheim, M.J., Miller, T.R., Zhang, Q. (2018) Method and apparatus for enhancing 3D model resolution. *United States Patent Application* 20190311461.

Mercuri, P.A., Engel, B.A., Johannsen, C.J. (2006) Evaluation and accuracy assessment of high-resolution IFSAR DEMs in low-relief areas. *International Journal of Remote Sensing*, 27(13), 2767–2786.

Miettinen, J., Shi, C., Liew, S.C. (2016) Land cover distribution in the peatlands of Peninsular Malaysia, Sumatra and Borneo in 2015 with changes since 1990. *Global Ecology and Conservation*, 6, 67–78.

Miettinen, J., Shi, C., Liew, S.C. (2017) Fire distribution in Peninsular Malaysia, Sumatra and Borneo in 2015 with special emphasis on peatland fires. *Environmental Management*, 60, 747–757.

Nasrul, B., Maas, A., Utami, S.N.H., Nurudin, M. (2020) The relationship between surface topography and peat thickness on Tebing Tinggi Island, Indonesia. *Mires and Peat*, 26, 18, 21 pp.

Neuzil, S.G. (1997) Onset and rate of peat and carbon accumulation in four domed ombrogenous peat deposits, Indonesia. In: Rieley J.O., Page, S.E. (eds.) *Biodiversity and Sustainability of Tropical Peatlands*. Samara Publishing Ltd., Cardigan, UK, 55–72.

Page S., Hoscilo, A., Langner, A., Tansey, K., Siegert, F., Limin, S., Rieley, J. (2009) Tropical peatland fires in Southeast Asia. In: Cochrane, M.A. (ed.) *Tropical Fire Ecology: Climate Change, Land Use, and Ecosystem Dynamics*. Springer Praxis Books, Springer, Berlin, 263–287.

Page, S.E., Rieley, J.O., Banks, C.J. (2011) Global and regional importance of the tropical peatland carbon pool. *Global Change Biology*, 17(2), 798–818.

Posa, M.R.C., Wijedasa, L.S., Corlett, R.T. (2011) Biodiversity and conservation of tropical peat swamp forests. *BioScience*, 61(1), 49–57.

Richards, M.A. (2007) A beginner's guide to Interferometric SAR concepts and signal processing. *Institute of Electrical and Electronics Engineers (IEEE) A&E Systems Magazine*, 22(9), 5–29.

Rizaldy, A., Mayasari, R. (2016) Acceleration of topographic map production using semi-automatic DTM from DSM radar data. XXIII ISPRS Congress, 12–19 July 2016, Prague, Czech Republic. *ISPRS - International Archives of the Photogrammetry, Remote Sensing and Spatial Information Sciences*, XLI-B7, 47–54.

Rudiyanto, R., Minasny, B., Setiawan, B., Saptomo, S.K., McBratney, A.B. (2018) Open digital mapping as a cost-effective method for mapping peat thickness and assessing the carbon stock of tropical peatlands. *Geoderma*, 313, 25–40.

Ruwaimana, M., Anshari, G.Z., Silva, L.C.R., Gavin, D.G. (2020) The oldest extant tropical peatland in the world: a major carbon reservoir for at least 47,000 years. *Environmental Research Letters*, 15, 114027, 10 pp.

Seymour, F., Samadhi, T.N. (2018) To save Indonesia's carbon-rich peatlands, start by mapping them. Blog dated 29 January 2018, World Resources Institute, Washington DC. Online at: https://www.wri.org/blog/2018/01/save-indonesias-carbon-rich-peatlands-start-mapping-them, accessed 29 Dec 2020.

Siegert, F., Ballhorn, U., Navratil, P., Joosten, H., Prayitno, M.B., Suroso, von Poncet, F., Manuri, S., Setiadi, B.B. (2018) *International Peat Mapping Team (IPMT) Presentation to the Public 02.02.2018, Pullman Hotel Jakarta (Indonesia)*. Online at: http://www.mongabay.co.id/wp-content/uploads/2018/02/Tim-Pemenang-Peat-

Prize.pdf, accessed 29 Dec 2020.

Supardi, Subekty, A.D., Neuzil, S.G. (1993) General geology and peat resources of the Siak Kanan and Bengkalis Island peat deposits, Sumatra, Indonesia. In: Cobb, J.C., Cecil, C.B. (eds.) *Modern and Ancient Coal-Forming Environments*, Special Paper 286, Geological Society of America, Boulder, Colorado, 45–61.

Sutikno, S., Sandhyavitri, A., Haidar, M., Yamamoto, K. (2017) Shoreline change analysis of peat soil beach in Bengkalis Island based on GIS and RS. *International Journal of Engineering and Technology*, 9(3), 233–238.

Tacconi, L. (2016) Preventing fires and haze in Southeast Asia. *Nature Climate Change*, 6(7), 640–643.

Tadono, T., Ishida, H., Oda, F., Naito, S., Minakawa, K., Iwamoto, H. (2014) Precise global DEM generation by ALOS PRISM. *International Society for Photogrammetry and Remote Sensing (ISPRS) Annals of the Photogrammetry, Remote Sensing and Spatial Information Sciences*, 2.4, 71–76.

Takaku, J., Tadono, T., Tsutsui, K., Ichikawa, M. (2016) Validation of 'AW3D' global DSM generated from ALOS PRISM. *International Society for Photogrammetry and Remote Sensing (ISPRS) Annals of the Photogrammetry, Remote Sensing and Spatial Information Sciences*, 3.4, 25–31.

Tata, H.L. (2019) Mixed farming systems on peatlands in Jambi and Central Kalimantan provinces, Indonesia: should they be described as paludiculture? *Mires and Peat*, 25, 08, 17 pp.

Thorburn, C.C., Kull, C.A. (2015) Peatlands and plantations in Sumatra, Indonesia: complex realities for resource governance, rural development and climate change mitigation. *Asia Pacific Viewpoint*, 56(1), 153–168.

Uda, S.K., Hein, L., Sumarga, E. (2017) Towards sustainable management of Indonesian tropical peatlands. *Wetlands Ecology and Management*, 25(6), 683—701.

Vernimmen, R., Hooijer, A., Akmalia, R., Fitranatanegara, N., Mulyadi, D., Yuherdha, A., Andreas, H., Page, S. (2020) Mapping deep peat carbon stock from a LiDAR based DTM and field measurements, with application to eastern Sumatra. *Carbon Balance and Management*, 15, 1–18.

Wahyunto, Suryadiputra, I.N.N. (2008) *Peatland Distribution in Sumatra and Kalimantan - Explanation of its Data Sets Including Source of Information, Accuracy, Data Constraints and Gaps*. Wetlands International - Indonesia Programme, Bogor, xiii+52 pp. Online at: https://indonesia.wetlands.org/publications/peatland-distribution-in-sumatra-and-kalimantan-explanation-of-its-data-sets-including-source-of-information-accuracy-data-constraints-and-gap/, accessed 29 Dec 2020.

Warren, M., Hergoualc'h, K., Kauffman, J.B., Murdiyarso, D., Kolka, R. (2017) An appraisal of Indonesia's immense peat carbon stock using national peatland maps: uncertainties and potential losses from conversion. *Carbon Balance and Management*, 12(1), 12, 12 pp.

Wijedasa, L.S., Jauhiainen, J., Könönen, M., Lampela and 135 others (2017) Denial of long-term issues with agriculture on tropical peatlands will have devastating consequences. *Global Change Biology*, 23(3), 977–982.

Zakaria, A. (2017) Application of Ifsar technology in topographic mapping: JUPEM's experience. *Proceedings of the International Cartographic Association*, 1, 125, 4 pp.

Zan, F.D., Guarnieri, A.M. (2006) TOPSAR: Terrain Observation by Progressive Scans. *Institute of Electrical and Electronics Engineers (IEEE) Transactions on Geoscience and Remote Sensing*, 44(9), 2352–2360.

Submitted 30 Nov 2019, revision 13 Oct 2020
Editors: Katherine H. Roucoux and Olivia Bragg

Author for correspondence: Earl Saxon, PhD, FRGS, 1718 P St. NW, #804, Washington DC 20036, USA.
Tel: +1.202.316.9084; E-mail: earl.saxon@forestinform.com

Data availability: the peat surface DTM and the peat base DPBM for each study site are available on request.

Supplementary material: a 3D video visualisation of the peat surface, peat base and peat soil sample columns at Kubu Raya is provided as a .mp4 file.

Appendix

Table A1. Accuracy of the DTM at Bengkalis by comparison with surveyed Ground Control Points (GCPs); (1) after standard processing from an IFSAR DSM and (2) after further processing to include ongoing peat surface dynamics and exclude man-made structures.

WGS 1984 UTM Zone 48N		Surveyed GCP	(1) DTM using IFSAR standards		(2) DTM adjusted to GCPs and edited for peat surface features	
Easting (m)	Northing (m)	Elevation (m)	Elevation (m)	Error (m)	Elevation (m)	Error (m)
328318	9952484	5.25	9.29	4.05	5.33	0.08
328334	9954576	4.49	10.97	6.49	4.51	0.02
331230	9954557	3.97	3.30	-0.67	3.80	-0.17
333636	9954766	4.51	9.09	4.58	4.48	-0.03
336613	9954737	7.29	7.19	-0.10	7.19	-0.10
339695	9954693	7.63	7.90	0.27	7.58	-0.05
336622	9952484	4.26	8.71	4.45	4.35	0.09
328298	9950657	3.81	4.94	1.13	3.82	0.01
325048	9951555	2.60	0.43	-2.18	2.54	-0.06
323083	9953430	2.26	1.62	-0.64	2.26	0.00
325328	9956026	2.32	0.68	-1.64	2.28	-0.04
328359	9956824	3.32	0.81	-2.51	3.26	-0.06
332189	9955828	3.21	3.30	0.10	3.30	0.09
336620	9956873	7.30	7.13	-0.17	7.32	0.02
339201	9958133	4.53	3.62	-0.90	4.48	-0.05
326741	9959060	3.44	2.61	-0.83	3.42	-0.02
339599	9950338	2.54	2.38	-0.16	2.58	0.04
333678	9949903	2.36	2.56	0.20	2.41	0.05
333437	9952470	3.10	2.79	-0.30	3.05	-0.05
321289	9950217	3.14	2.41	-0.73	3.08	-0.06
342083	9961530	2.82	3.57	0.75	2.92	0.10
345291	9956972	2.32	3.58	1.26	2.39	0.07
330604	9951379	2.28	2.45	0.17	2.14	-0.14
342509	9953442	1.97	1.26	-0.71	1.86	-0.11
342392	9957239	5.55	8.15	2.60	5.59	0.04
344113	9959155	2.56	3.25	0.69	2.48	-0.08
	M	3.80	4.38	0.59	3.79	-0.02
	SD	1.61	3.02	2.14	1.62	0.07
	RMSE			2.22		0.07

Table A2. Accuracy of the DTM at Kubu Raya by comparison with surveyed Ground Control Points (GCPs); (1) after standard processing from an IFSAR DSM and (2) after further processing to include ongoing peat surface dynamics and exclude man-made structures.

WGS 1984 UTM Zone 49S		Surveyed GCP	(1) DTM using IFSAR standards		(2) DTM adjusted to GCPs and edited for peat surface features	
Easting (m)	Northing (m)	Elevation (m)	Elevation (m)	Error (m)	Elevation (m)	Error (m)
201774	159211	2.62	3.72	1.10	2.63	0.01
199634	168325	3.16	3.60	0.44	3.19	0.03
217814	156210	2.15	2.37	0.22	2.16	0.01
207764	159871	2.55	3.58	1.03	2.72	0.17
211578	165250	6.99	6.96	-0.03	6.90	-0.09
216046	161534	2.49	1.71	-0.78	2.48	-0.01
220723	149748	2.45	2.60	0.15	2.52	0.07
221701	139588	2.42	3.51	1.09	2.50	0.08
203695	164412	8.02	8.97	0.95	8.01	-0.01
204417	154128	5.55	6.53	0.98	5.56	0.01
209537	147601	1.78	1.66	-0.12	1.86	0.08
211483	154767	7.89	9.58	1.69	8.08	0.19
204408	158942	4.08	3.59	-0.49	3.58	-0.50
201955	156847	3.37	3.69	0.32	3.74	0.37
216456	143384	3.30	3.52	0.22	3.52	0.22
214539	160777	3.57	3.67	0.10	3.72	0.15
210224	159584	3.39	3.89	0.50	3.63	0.24
210734	162165	3.65	3.36	-0.29	3.14	-0.51
219920	161936	3.00	2.86	-0.14	3.19	0.19
218966	164097	3.98	3.57	-0.41	3.59	-0.39
	M	3.82	4.15	0.33	3.84	0.02
	SD	1.80	2.11	0.63	1.79	0.23
	RMSE			0.71		0.23

Table A3. Surface fitting error in the 3D peat models.

Location	Peat thickness	Average peat thickness measured in soil cores (m)	Average peat thickness in the 3D model at soil core sites (m)	RMSE between measured and modelled peat thickness (m)
Bengkalis	shallow	1.28 ± 0.73	1.37 ± 0.72	0.16
	deep	8.12 ± 2.32	8.10 ± 2.29	0.11
Kubu Raya	shallow	1.40 ± 0.88	1.39 ± 0.88	0.09
	deep	5.40 ± 1.19	5.39 ± 1.21	0.07

Table A4. Sampling error in the 3D peat models.

Location	Peat thickness	Average peat thickness measured in soil cores (m)	Average peat thickness across the entire peat model (m)	Difference between measured and modelled peat thickness (m)	(z-score)
Bengkalis	shallow	1.28 ± 0.73	1.82 ± 0.76	-0.54	0.71
	deep	8.12 ± 2.32	7.64 ± 2.34	0.48	0.21
Kubu Raya	shallow	1.40 ± 0.88	1.48 ± 0.74	-0.08	0.11
	deep	5.40 ± 1.19	4.86 ± 1.24	0.54	0.44